Advances in Nano Research, *Vol. 19, No. 5 (2025) 519-530*
https://doi.org/10.12989/anr.2025.19.5.519

Auxetic microrods for vibration control: Toward next-generation shin guard design

Chao Pan*[1] and Mostafa Habibi[2,3]

[1]*Hunan Mass Media Vocational and Technical College, Changsha 410100, Hunan, China*
[2]*Department of Biomaterials, Saveetha Dental College and Hospital, Saveetha Institute of Medical and Technical Sciences, Chennai, India*
[3]*Department of Mechanical Engineering, Faculty of Engineering, Haliç University, Istanbul, Turkey*

(*Received April 7, 2025, Revised October 21, 2025, Accepted November 13, 2025*)

Abstract. This study explores the behavior of auxetic microrods—unusual structures that expand sideways when stretched—under torsional vibration. We examined triangular and elliptical forms using nonlocal strain gradient theory to capture the subtle effects that appear at very small scales. The analysis shows that shape, orientation, and boundary support all play a decisive role in how these rods respond. Although the work is grounded in mechanics, the findings translate readily into sports applications. Shin guards, for instance, face repeated, high-energy impacts where comfort and protection often pull in opposite directions. Traditional foams and plastics tend to pass sharp vibrations into the leg or wear out quickly. Auxetic microrods, by contrast, can spread the force of a strike, soften the shock, and extend the life of the gear—all without adding bulk. Incorporating these microscale structures could give athletes shin guards that are lighter, tougher, and more comfortable, marking a clear step toward smarter protective equipment.
Keywords: analytical method; auxetic microrod; elliptical cross-section; NSGT; shin guard

1. Introduction

The need for strong, lightweight materials with a wide range of applications has spurred significant advancements in recent decades, resulting in the development of new composites and innovative material technologies (Wang *et al*. 2021, Zhang *et al*. 2025, Zhao *et al*. 2024). Composite materials, which are composed of individual parts, have garnered significant interest due to their high strength-to-weight ratio, hardness, and corrosion resistance. They are extensively utilized in the biomedical, automotive, marine, and aerospace sectors. (Alghanmi, 2025, Boulahbal *et al*. 2025, Palani and Swain, 2025, Qin *et al*. 2020). Functionally graded materials (FGM), which were first developed in Japan in the 1980s, have attracted much attention among various composite materials because they can smoothly change composition or microstructure, effectively reducing stress concentration and interfacial delamination that often occur in conventional multilayer composites (Gartia and Chakraverty, 2025, Koizumi, 1997, Liu *et al*. 2021a, b). Also, the use of carbon nanotubes and graphene as nanofillers significantly enhances the mechanical performance, heat transfer, and vibration damping of these advanced composite materials (Alkunte *et al*. 2024a, b, Kavousi Sisi *et al*. 2025, Qin *et al*. 2020).

Considering the wide application of these materials and the global need for these materials, researchers have conducted many analytical and numerical studies on the static and dynamic behavior of FG nanostructures or microstructures, including beams, rods, plates, and shells (Challamel *et al*. 2025, Huang *et al*. 2025, Liu *et al*. 2022, Wang *et al*. 2025, Yuanchao *et al*. 2025b). For example, Qin *et al*. (2020) offered a complete solution for the vibration analysis of graphene-reinforced graded thin shells subjected to general boundary conditions. Faghidian and Tounsi (2022) presented an innovative numerical criterion for the dynamic analysis of nanostructures utilizing hybrid gradient theory, along with an extensive investigation of the dynamic behavior of elastic nanobeams. Also, Xiao *et al*. (2024) investigated wave propagation in porous FG bio-omposite beams on elastic media and showed that porosity and base properties can play important roles in frequency and wave velocity. Similarly, the investigation of wave propagation in porous biocomposite beams FG has been conducted, considering the effects of porosity and foundation (Yuanchao *et al*. 2025a). Another group of researchers used high-order, nonlocal shear theories to analyze fg plates and shells (Bousmaha *et al*. 2025, Cuong-Le *et al*. 2022, Liu *et al*. 2022, Van Vinh and Tounsi, 2022b). Van Vinh and Tounsi (2022a) studied the free vibration of FG doubly curved nanoshells using the nonlocal first-order shear deformation theory with variable nonlocal parameters. Later Van Vinh and Zenkour (2025) analyzed the vibration of porous FG sandwich plates on viscoelastic and Winkler-Pasternak foundations under different boundary conditions. Their numerical findings indicated that the damped frequency drops quickly as damping coefficients increase. The response of piezoelectric FG shells to nonlinear forced vibrations under thermo-mechanical and electrical loading was investigated by Liu *et al*. (2021b), Electroelastic analysis of piezoelectric curved nanoshells employing

*Corresponding author, Ph.D.,
E-mail: panchao79@126.com

ISSN: 2287-237X (Print), 2287-2388 (Online)

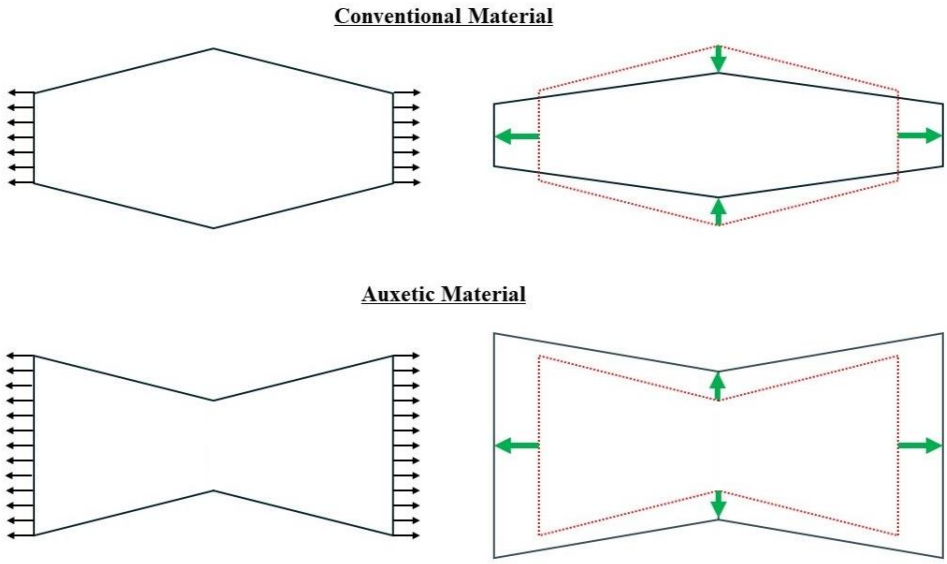

Fig. 1. The assessment of mechanical response of auxetic and conventional materials subjected to tensile load

Eringen's nonlocal elasticity theory (ENET) has demonstrated that size influences vibrational behavior and stress distribution (Zhu *et al*. 2025). In addition, Li *et al*. (2025) created a new mathematical model based on higher-order shear deformation to study the vibration of a doubly curved shell. Wave propagation and bending analysis in FG plates have also been examined through analytical methods and quasi-3D theories (Boussalem *et al*. 2025, Fang *et al*. 2025, Yang *et al*. 2025). In addition, several studies have used other scale-dependent theories like the nonlocal strain gradient theory (NSGT), the modified coupled stress theory, and the Two-Helmholtz NSGT (Bağdatlı, 2015, Ebrahimi *et al*. 2019, Gheshlaghi and Hasheminejad, 2011, Pradhan and Phadikar, 2009). For example, Arefi and Amabili (2021) used ENET to examine the bending and stability characteristics of bilayer MEE nanoshells with dual curvature subjected to in-plane magnetic, electrical, and mechanical force. Zarezadeh *et al*. (2020) examined how FG nanorods vibrate torsionally on a torsional medium in a magnetic field using ENET. Jankowski *et al*. (2020) studied the dynamic behavior and stability of imperfect nanoscale beams using HSDT and NSGT. Despite significant progress in the development of FG materials, studies show that, although they offer many structural advantages, they still have limitations in vibration absorption and energy dissipation under severe dynamic conditions. These limitations led to the introduction of auxetic materials as a new class. auxetic materials are a new class of materials that exhibit a negative Poisson's ratio. Unlike conventional materials that contract laterally, auxetic materials expand in the transverse direction. This feature not only increases energy absorption, mechanical resistance to indentation, and vibration reduction but also helps address the structural weakness of traditional FG materials and improves dynamic performance. Fig. 1 below shows how conventional and auxetic materials perform differently under tension to help readers understand these differences (Hu *et al*. 2025, Seyfi *et al*. 2024).

Researchers have studied auxetic structures using different mechanical analyses, including buckling, vibration, and wave propagation, because of their unique mechanical behavior (Beitollahi *et al*. 2025, Kadiri *et al*. 2024, Nasrekani *et al*. 2025). For example, Hajmohammad *et al*. (2019) investigated the free vibration behavior of sandwich plates featuring an auxetic honeycomb core and dense composite overlays. These plates were positioned on a viscoelastic medium and subjected to magnetic fields and blast loads, all analyzed using the sinusoidal shear deformation theory (SSDT). The nonlinear dynamic and static responses of laminated beams with an auxetic FG core under thermal conditions were evaluated by Li *et al*. (2018, 2019). Eipakchi and Mahboubi Nasrekani (2020) conducted the free vibration analysis of a composite sandwich shell with an auxetic core under moving internal pressure. Recent findings by Hu *et al*. (2025) indicate that a polygonal metamaterial with auxetic behavior improves stress dispersion capability and is considered a suitable option for structural systems requiring high impact resistance. Also, research has indicated that auxetic nano-composites, as well as other nanostructured auxetic materials, offer valuable functionalities in both athletic and medical fields (Chang *et al*. 2025, Dai *et al*. 2022, Liu *et al*. 2025, Xia *et al*. 2025, YaJie *et al*. 2025, Yu *et al*. 2023). For instance, adding graphene oxide to volleyballs improves their vibration stability and energy dissipation (Daichang *et al*. 2025, Xu *et al*. 2025). Polymer nanocomposites with nanoclay and wood powder have also made helmets and sports equipment stronger (Yang *et al*. 2025). Chen *et al*. (2025) investigated how exercise impacts protein tissue stability in athletes by using biomechanical analysis with size-related models. Their findings indicated that physical activity can markedly affect the mechanical properties of tissues and fibers. In a related study, Chen *et al*. (2025) looked at how physical exercise impacts the stability of nanodevices used for targeted drug delivery. They used a modeling method that combines higher-order beam theory

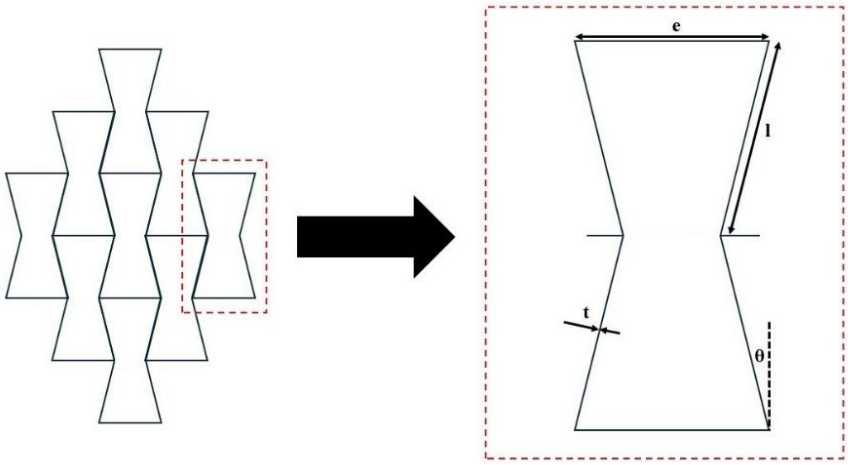

Fig. 2 Cell geometry of the auxetic honeycomb core

with NSGT to simulate nanodevices with uneven tubular shapes. The findings show that hydrodynamic forces during exercise can affect the stability of nanodevices. To improve outcomes in sports medicine and rehabilitation, it is important to consider both mechanical design and physiological conditions. Wan *et al*. (2025) also studied small-scale rotational structures like nanobeams and nanotubes for advanced sports equipment. Their results show that these structures reduce vibration and improve endurance. The structures also have different acousto-optic shapes, each with its own way of changing form. The researchers demonstrated that lightweight hollow constructions with graded performance exhibit superior strength-to-weight ratios and stability. This aids in the construction of high-performance apparatus such as bicycle frames, ski poles, and gymnastic bars (Xiao *et al*. 2025). ENET in its integral version has been shown to create paradoxes and poorly defined boundary problems in some cases. This work uses the Nonlocal Strain Gradient Theory (NSGT) to get around these problems. NSGT efficiently integrates nonlocal and strain-gradient effects, guaranteeing theoretically stable and physically coherent modeling of size-dependent behavior in torsional vibration. This approach allows capturing both the long-range interatomic interactions and the microstructural stiffness variations without the inconsistencies observed in the conventional ENET. Despite extensive studies on auxetic nano- and microstructures, scale-dependent torsional vibration in circular microrods has not been investigated to date, therefore, the present study aims to address this scientific gap. For the first time, this study presents an analytical approach for the torsional vibration of auxetic microrods with non-circular cross-sections that models small-scale effects using NSGT. While previous studies focused on FG nanorods with circular cross-sections, this innovative model demonstrates that combining non-circular cross-sectional geometry with auxetic behavior can effectively control the stiffness-frequency relationship at the microscale. The findings indicate that the cross-sectional geometry and auxetic behavior jointly determine the stiffness-frequency relationship at the microscale.

This study examines the torsional oscillation of non-circular auxetic microrods made from thermoplastic polyurethane with elliptical and triangular cross-sections. NSGT is used to include small-scale effects, and the system's equations are based on Hamilton's principle. While torsion-flexure coupling can happen in non-circular cross-sections, it is not considered here because the boundary conditions are symmetrical and the geometry is uniform. An analytical method is used to solve the non-local equations, and the study looks at how different parameters affect the torsional frequency of these honeycomb auxetic microrods.

2. Theory and formulation

In this research, a reform-auxetic honeycomb serves as the fundamental material for the microrod. One of the key benefits of this research is the application of auxetic material. Different parameters of the auxetic unit are displayed in Fig. 2. In Fig. 2, θ denotes the angle of inclination, and the impact of this crucial parameter is extensively analyzed in the results section. The lengths of the horizontal and inclined edges of the auxetic cell are denoted by e and l, respectively.

The effective properties of auxetic materials are obtained in terms of elastic modulus (*E*), shear modulus (G), density (ρ), and Poisson's ratio (ν) (QING and ZHI, 2010):

$$\begin{Bmatrix} E_a = E\left(\frac{t}{l}\right)^3 \frac{\cos\theta}{\left(\sin\theta + \frac{e}{l}\right)\sin^2\theta} \\ G_a = E\left(\frac{t}{l}\right)^3 \frac{\left(\frac{e}{l} + \sin\theta\right)}{\left(\frac{e}{l}\right)^2\left(1 + \frac{2e}{l}\right)\cos\theta} \\ \rho_a = \rho\frac{\frac{t}{l}\left(2 + \frac{e}{l}\right)}{2\cos\ \theta\left(\sin\theta + \frac{e}{l}\right)} \\ v_a = \frac{\cos^2\theta}{\left(\sin\theta + \frac{e}{l}\right)\sin\theta} \end{Bmatrix} \quad (1)$$

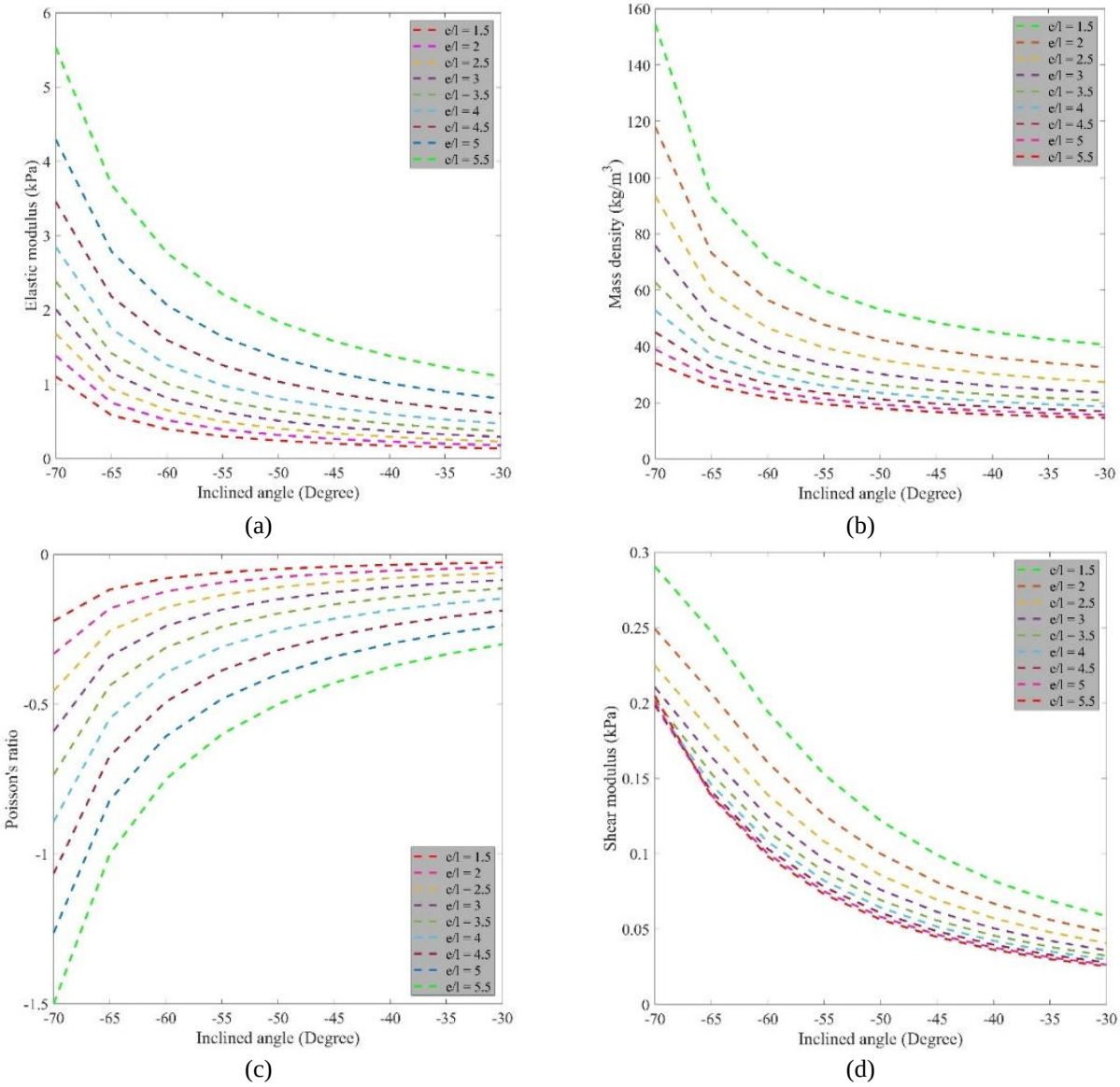

Fig. 3 Variation of (a) Elastic modulus (b) mass density (c) Poisson's ratio (d) shear modulus versus incline angle for different e/l

To show how $\frac{e}{l}$ and inclined angle affect properties of auxetic material, Fig. 3 is plotted. As the inclined angle becomes more negative, the elastic modulus, mass density, and shear modulus decrease, while Poisson's ratio increases. This behavior reflects the fact that a larger negative inclined angle intensifies the re-entrant geometry, making the structure more compliant and strongly auxetic. Furthermore, higher values of e/l lead to overall stiffer behavior, indicating the sensitivity of mechanical response to both geometric configuration and scale ratio.

Here, the values of $\frac{e}{l}$ and $\frac{t}{l}$ are considered to be 4 and 0.0138571, respectively.

2.1 Governing equations deriving

This model defines the displacement field of the auxetic rod in the x-direction for any point as follows:

$$u(x,t) = \psi(y,z)\theta_{,x}(x,t) \tag{2}$$

$$v(x,t) = -z\theta(x,t) \tag{3}$$

$$w(x,t) = y\theta(x,t) \tag{4}$$

where, u, v and w represent the x, y and z-displacement, respectively. Also, θ and ψ denote the microrod's twix angle and warping function, respectively. In this work, triangular and elliptical shapes are regarded for microrod's cross-section The warping functions of the mentioned shapes are expressed in the following form (Sokolnikoff and Specht, 1956):

$$\psi_{tr}(y,z) = \frac{y}{6\xi}(3z^2 - y^2) \tag{5}$$

$$\psi_{el}(y,z) = \left(\frac{b^2 - a^2}{b^2 + a^2}\right)yz \tag{6}$$

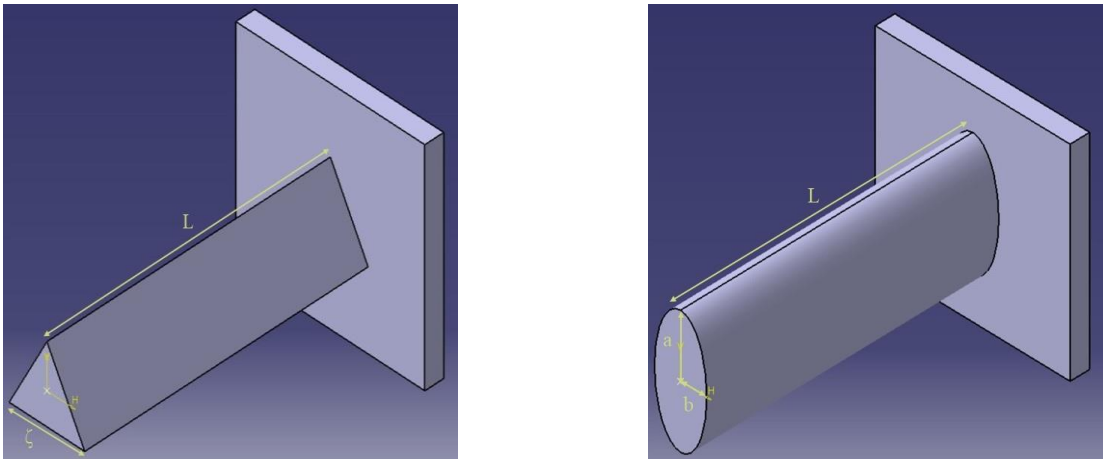

(a) (b)

Fig. 4 Schematic of microrod with non-circular cross-section (a) triangular (b) elliptical

Subscripts *tr* and *el* state triangular and elliptical shape, respectively. Also, $\xi = \frac{\sqrt{3}\,\zeta}{6}$. To enhance readers' comprehension, a diagram of non-circular microrods is included in Fig. 4.

It is worth noting that for non-circular cross-sections, torsion–flexure coupling may occur due to geometric asymmetry. However, in the present analysis, pure torsion is assumed since the boundary conditions are symmetric and the geometry is uniformly distributed along the length. Under these conditions, flexural deformation is suppressed, and torsional vibration dominates the response.

The non-zero elements of the strain fields is written as:

$$\varepsilon_{xy} = u_{,y} + v_{,x} = \left(\psi_{,y} - z\right)\theta_{,x} \tag{7}$$

$$\varepsilon_{xz} = u_{,z} + w_{,x} = \left(\psi_{,z} + y\right)\theta_{,x} \tag{8}$$

Hamilton's principle is used to derive the governing equation for torsional vibration over the time interval from 0 and *t*:

$$\int_0^t [\delta U - (\delta T + \delta W)]dt = 0 \tag{9}$$

in which, *U*, *T*, and *W* denote strain and kinetic energies, and work done by external forces, respectively. The strain energy's variation is written as:

$$\begin{aligned}\delta \int_0^t U dt &= \int_0^t \int_V \sigma_{ij}\delta\varepsilon_{ij} dV \\ &= \int_V \left(\sigma_{xz}\delta\varepsilon_{xz} + \sigma_{xy}\delta\varepsilon_{xy}\right)dV\end{aligned} \tag{10}$$

Replacing Eqs. (7) – (8) into above equation leads to:

$$\begin{aligned}\delta \int_0^t U dt = \int_0^t \int_0^L \left\{\left(M^T \frac{\partial\delta\theta}{\partial x}\right)dxdt \right. \\ \left. + \int_0^L \int_A \left(\sigma_{xy}\frac{\partial\delta\psi(y,z)}{\partial y} + \sigma_{xz}\frac{\partial\delta\psi(y,z)}{\partial z}\right)\theta_{,x} dA dx\right\} dt\end{aligned} \tag{11}$$

The torsional torque's moment is written as:

$$\begin{aligned}M^T = \int_A \Big(\sigma_{xy}\left(\psi_{,y}(y,z) - z\right) \\ + \sigma_{xz}\left(\psi_{,z}(y,z) + y\right)\Big)\, dA\end{aligned} \tag{12}$$

Eq. (11) is rewritten as:

$$\delta \int_0^t U dt = \int_0^t \left(M^T|_0^L - \int_0^L M^T_{,x}\,\delta\theta dx\right) dt \tag{13}$$

Kinetic energy's variation is stated as:

$$\begin{aligned}T = \frac{1}{2}\int_V \rho\left\{\psi^2(y,z)\left(\dot{\theta}_{,x}\right)^2 + (-zt)^2 + \left(y\dot{\theta}\right)^2\right\}dV \\ = I_a + I_b\end{aligned} \tag{14}$$

where, I_a and I_b denote respectively axial inertia and polar inertia, and they are formulated as:

$$I_a = \frac{1}{2}\int_0^L \int_A \rho\psi^2(y,z)\dot{\theta}^2_{,x} dA dx \tag{15}$$

$$I_b = \frac{1}{2}\int_0^L \rho I_p \dot{\theta}^2 dx = \frac{1}{2}\int_0^L I_o \dot{\theta}^2 dx \tag{16}$$

where in Eq. (16), mass and polar moment of inertias (I_o and I_p) are presented as:

$$I_o = \rho \int_A (y^2 + z^2) dA = \rho I_p \tag{17}$$

$$I_p = \int_A (y^2 + z^2) dA \tag{18}$$

The variations of moments of inertia are derived as:

$$\delta \int_0^t I_a = \int_0^t \int_0^L \rho I_\psi \ddot{\theta}_{,xx}\delta\theta dx dt - \int_0^t \rho I_\psi \ddot{\theta}_{,x}\delta\theta\Big|_0^L dt \tag{19}$$

$$\delta \int_0^t I_b = \int_0^t I_o \left(\dot{\theta}\delta\theta\big|_0^L - \int_0^L \ddot{\theta} dx\right) \tag{20}$$

Table 1 The dimensionless frequencies of the clamed auxetic microscale rod with triangular cross-section for dissimilar triangle edges and nonlocal parameters (l = 15 nm)

μ (nm)	Triangle edges					
	ζ = 1 (nm)		ζ = 5 (nm)		ζ = 10 (nm)	
	Liu *et al*. (2025)	Present	Liu *et al*. (2025)	Present	Liu *et al*. (2025)	Present
0	2.4331	2.4333	2.4298	2.4301	2.4203	2.4208
1	2.3813	2.3815	2.3782	2.3786	2.3690	2.3694
1.5	2.3211	2.3212	2.3180	2.3185	2.3092	2.3093
2	2.2439	2.2441	2.2410	2.2415	2.2322	2.2325

where

$$I_\psi = \int_A \psi^2(y,z)dA \tag{21}$$

No external force is applied in this research and because of this, the variation of work done is ignored. By replacing Eqs. (13) and (14) into Eq. (9), the relations of motion and the boundary condition (B.C) are derived as:

$$M^T_{,x} = I_o\theta_{,tt} - \rho I_\psi \ddot{\theta}_{,xx} \tag{22}$$

$$\left(M^T + \rho I_\psi \ddot{\theta}_{,x}\right)\Big|_0^L = 0 \quad or \quad \delta\theta|_0^L = 0 \tag{23}$$

The following equation introduces the constitutive relation of auxetic microrod based on NSGT in terms of nonlocal parameter and length-scale parameter:

$$(1-\mu^2\nabla^2)\sigma_{ij} = (1-\eta^2\nabla^2)C:\varepsilon_{ij} \quad ij = xz, xy \tag{24}$$

Next, the following equation is nonlocal dynamic equation:

$$(1-\mu^2\nabla^2)M^T = (1-\eta^2\nabla^2)G\left(\int_A \left(\psi_{,y}-z\right)^2 + \left(\psi_{,z}+y\right)^2 dA\right)\theta_{,x} \tag{25}$$

By simplifying the coupled Eq. (22) with Eq. (25), the nonlocal governing equation of the auxetic microrod is written as follows:

$$(1-\eta^2\nabla^2)G\left(\int_A \left(\psi_{,y}-z\right)^2 + \left(\psi_{,z}+y\right)^2 dA\right)\theta_{,xx} + \rho I_\psi \ddot{\theta}_{,xx} - I_o\ddot{\theta} + \mu^2\left(I_o\ddot{\theta}_{,xx} - \rho I_\psi \ddot{\theta}_{,xxxx}\right) = 0 \tag{26}$$

3. Solution procedure

This section provides a general solution for extracting the numerical results of the calculated formulation:

$$\theta(x,t) = \sum_{m=1}^{\infty} \Theta_m(x)e^{i\omega_m t} \tag{27}$$

where, Θ_m states the mth mode shape, which for two dissimilar B.C can be written in the following form:

$$\Theta_m = \chi_m sin\,(\Gamma x) \tag{28}$$

The parameter Γ for B.Cs, Clamped-Clamped (C-C) and Clamped–Free (C-F), is computed as:

$$\Gamma = \begin{cases} \dfrac{m\pi}{L} & C-C \\ \dfrac{(2m-1)\pi}{2L} & C-F \end{cases} \tag{29}$$

By applying Eq. (27) into Eq. (26), the torsional frequency of auxetic microrod is obtained.

4. Numerical results

Here, the oscillation of the non-circular auxetic microrods under different boundary conditions is evaluated in several figures. The impacts of various variants on variations in torsional frequency are examined and shown below. Additionally, the dimensionless frequencies of the current model are compared with those from similar studies, and the outcomes are provided.

4.1 Validation

In the present analysis, the nonlocal parameter μ represents the material's internal length-scale effect, which accounts for atomic-level interactions within the ENET framework. The choice of μ values is based on earlier studies of micro- and nano-scale torsional vibration (Arda, 2021, Faghidian and Tounsi, 2022, Zarezadeh *et al*. 2020), where μ usually ranges from 0 to 10 μm for metallic and composite materials at the microscale. When μ is 0, it represents classical local elasticity. When μ values are higher, nonlocal effects become stronger and this reduces the structural stiffness. In this study, we use μ values from 2 to 10 μm to examine how small-scale interactions affect the dynamic response of auxetic microrods.

Table 1 compares the dimensionless fundamental natural frequencies of a C-C boundary condition auxetic triangular microwire across different nonlocal parameter (μ) values and triangle edge lengths (ζ). The results align closely with those of Liu *et al*. (2025), with a maximum deviation of 0.1%. This strong agreement validates the NSGT-based analytical method's capability to accurately model the dynamic behavior of auxetic microrods. Furthermore, the observed decrease in natural frequency as μ increases underscores the role of nonlocal effects in diminishing structural stiffness.

The verification of the dimensionless frequencies of the clamped elliptical microrod with varying b/a ratios and nonlocal parameters (l = 20 nm) is shown in Table 2. The current results are very similar to those reported by J. Liu *et al*. (2025), with differences of less than 0.1%. This confirms that the approach is reliable. As the nonlocal parameter μ increases, the natural frequency decreases. This indicates a stiffness-softening effect related to small-scale phenomena. Additionally, changing the cross-sectional ratio a / b significantly influences the dynamic response, higher a / b ratios result in greater bending stiffness and, consequently,

Table 2 The verification of the dimensionless frequencies of the clamped elliptical microrod for the dissimilar nonlocal parameters and a/b ratios (l = 20 nm)

μ (nm)	Cross-section ratio					
	a/b = 0.1		a/b = 1		a/b = 10	
	Liu *et al*. (2025)	Present	Liu *et al*. (2025)	Present	Liu *et al*. (2025)	Present
0	0.6212	0.6214	3.1273	3.1273	0.6220	0.6220
1	0.6137	0.6139	3.0893	3.0894	0.6144	0.6145
1.5	0.6046	0.6048	3.0438	3.0439	0.6053	0.6054
2	0.5925	0.5928	2.9832	2.9834	0.9533	0.5934

Table 3 Torsional frequency (kHz) versus incline angle and m for different boundary condition and cross-sections

Cross-section	Boundary condition	m	Incline angle				
			-30	-40	-50	-60	-70
Triangular	C-C	1	76.4362	73.3179	70.6261	68.4426	66.8338
		2	138.0340	132.4027	127.5416	123.5985	120.6932
		3	182.7552	175.2995	168.8635	163.6429	159.7963
		4	215.6275	206.8306	199.2370	193.0774	188.5389
	C-F	1	39.3985	37.7912	36.4037	35.2782	34.4490
		2	109.5082	105.0407	101.1842	98.0560	95.7511
		3	162.2372	155.6185	149.9051	145.2706	141.8559
		4	200.3275	192.1548	185.1001	179.3775	175.1611
Elliptical	C-C	1	87.1488	83.5935	80.5244	78.0349	76.2006
		2	157.8064	151.3685	145.8111	141.3032	137.9818
		3	209.8582	201.2967	193.9063	187.9115	183.4945
		4	249.0905	238.9285	230.1564	223.0409	217.7981
	C-F	1	44.8895	43.0581	41.4773	40.1950	39.2502
		2	124.9976	119.8981	115.4962	111.9255	109.2946
		3	185.8483	178.2664	171.7215	166.4125	162.5009
		4	230.6826	221.2715	213.1478	206.5581	201.7027

higher natural frequencies. The results indicate that the proposed analytical model reliably and accurately predicts the vibration of non-circular auxetic microrods.

Tables 1 and 2 show that a rod's cross-sectional shape has a big impact on its performance. Elliptical rods spread stress more evenly and are stiffer, which leads to higher natural frequencies and less deformation. In contrast, triangular rods collect stress at their corners, causing local deformation and making them more sensitive in some vibrational modes. This research demonstrates that the geometry of the cross-section significantly influences a structure's response, irrespective of material and dimensions being constant.

4.2 Numerical example

A numerical example was used to further test the proposed analytical model and to study how geometry and boundary constraints affect the results. In this example, the torsional natural frequencies of auxetic microrods with triangular and elliptical cross-sections were analyzed under two boundary conditions: C–C and C–F.

The variations of torsional frequency (kHz) with different tlt angles (-30° to -70°) and four vibration modes (m = 1-4) for various boundary conditions and cross sections are shown in Table 3. The results show the natural frequency diminishes with an increase in the incline angle. The reason for this pattern is that the rod's effective torsional rigidity gets weaker as you move along its axis. This is because larger angles cause the shear stress to be less evenly distributed and the strain to be more concentrated in some areas. Also, as expected, higher vibration modes mean higher frequencies. This means more energy and more complex patterns of deformation. A comparison of the two boundary conditions reveals that C–C configurations have higher frequencies than C–F configurations because the stronger end constraints increase the system's overall stiffness. Moreover, elliptical microrods generally demonstrate higher torsional frequencies than triangular ones due to their larger polar moment of inertia and more uniform stress distribution.

Fig. 5 shows how the natural frequency varies with the length-scale parameter for different nonlocal parameters (μ = 2, 4, 6, 8, and 10 μm). Two cross-sectional geometries-elliptical and triangular—were analyzed under C–C and C–F boundary conditions. In every case, the natural frequency

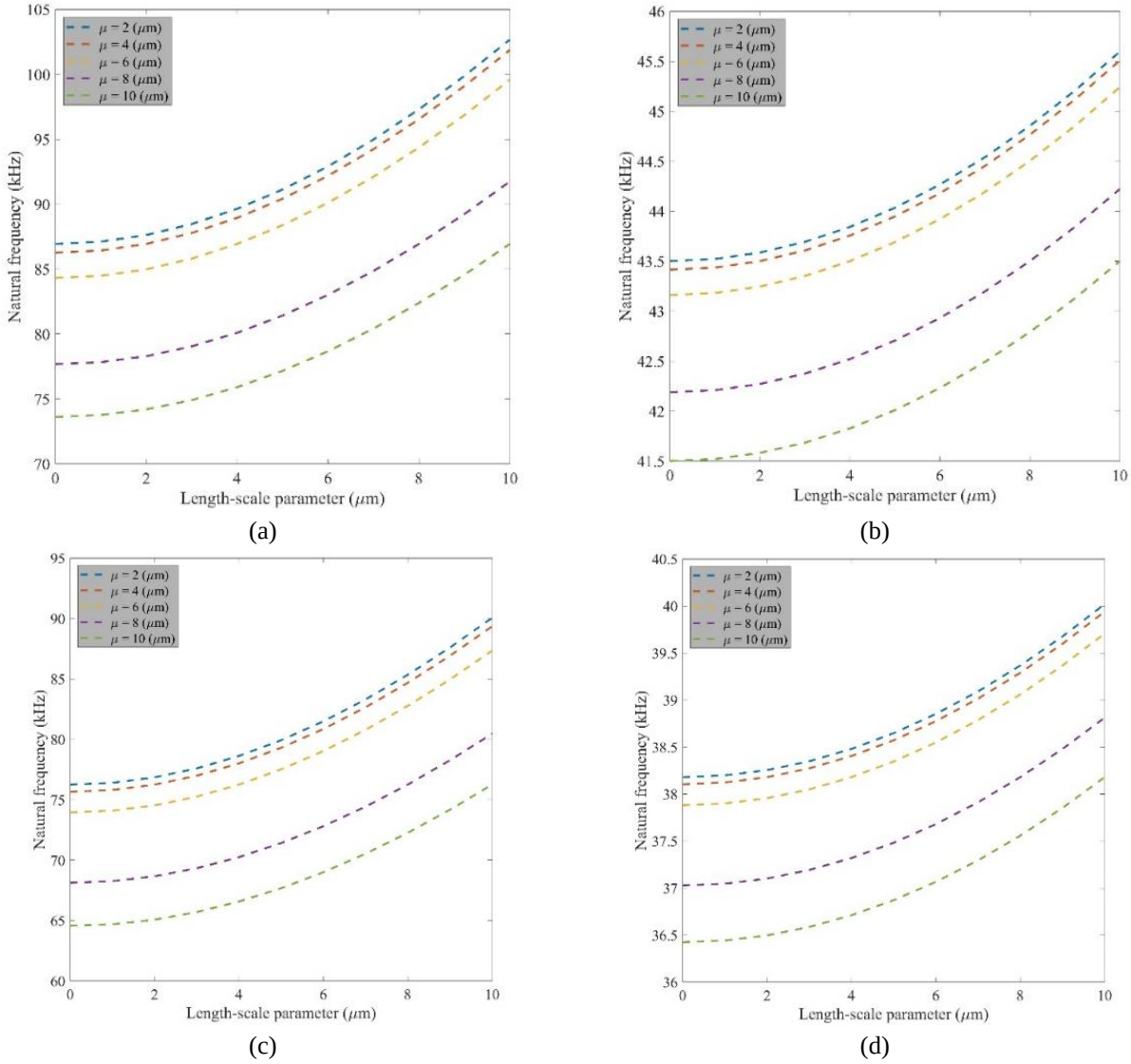

Fig. 5 Variation of the natural frequency versus length-scale parameter for various nonlocal parameters for elliptical cross-section under (a) C-C (b) C-F boundary conditions and triangular cross-section (c) C-C (d) C-F boundary conditions

increases as the length-scale parameter gets larger, showing a clear size-dependent effect described by the nonlocal strain gradient theory. As the microstructural characteristic length grows, the material becomes stiffer, which leads to higher natural frequencies. When comparing the two cross-sections, the elliptical microrod shows slightly higher natural frequencies than the triangular one because its shape is smoother and its moment of inertia is higher. In the same way, the C-C boundary condition leads to higher frequencies than the C-F case because both ends are more strongly constrained.

Fig. 6 presents the variation in the natural frequency with microrod length for different geometric parameters and boundary conditions. Both elliptical and triangular cross-sections are analyzed under C–C and C–F configurations. As you can see, the natural frequency decreases sharply with increasing microrod length, particularly at shorter lengths. This inverse relationship indicates that shorter rods have higher stiffness and therefore exhibit higher natural frequencies, whereas longer rods exhibit lower stiffness and lower natural frequencies. For the elliptical microrod, the aspect ratio (a/b) greatly influences its behavior: higher aspect ratios lead to higher frequencies because of increased bending stiffness along the central axis. The triangular cross-section follows a similar pattern but has slightly lower frequency values, which is due to its smaller second moment of area. As expected, the C–C boundary condition always results in higher frequencies than the C–F condition. This confirms that supports with more constraints increase stiffness and resistance to vibration.

5. Conclusions

This study examines the behavior of auxetic microrods unusual structures that expand laterally when stretched—

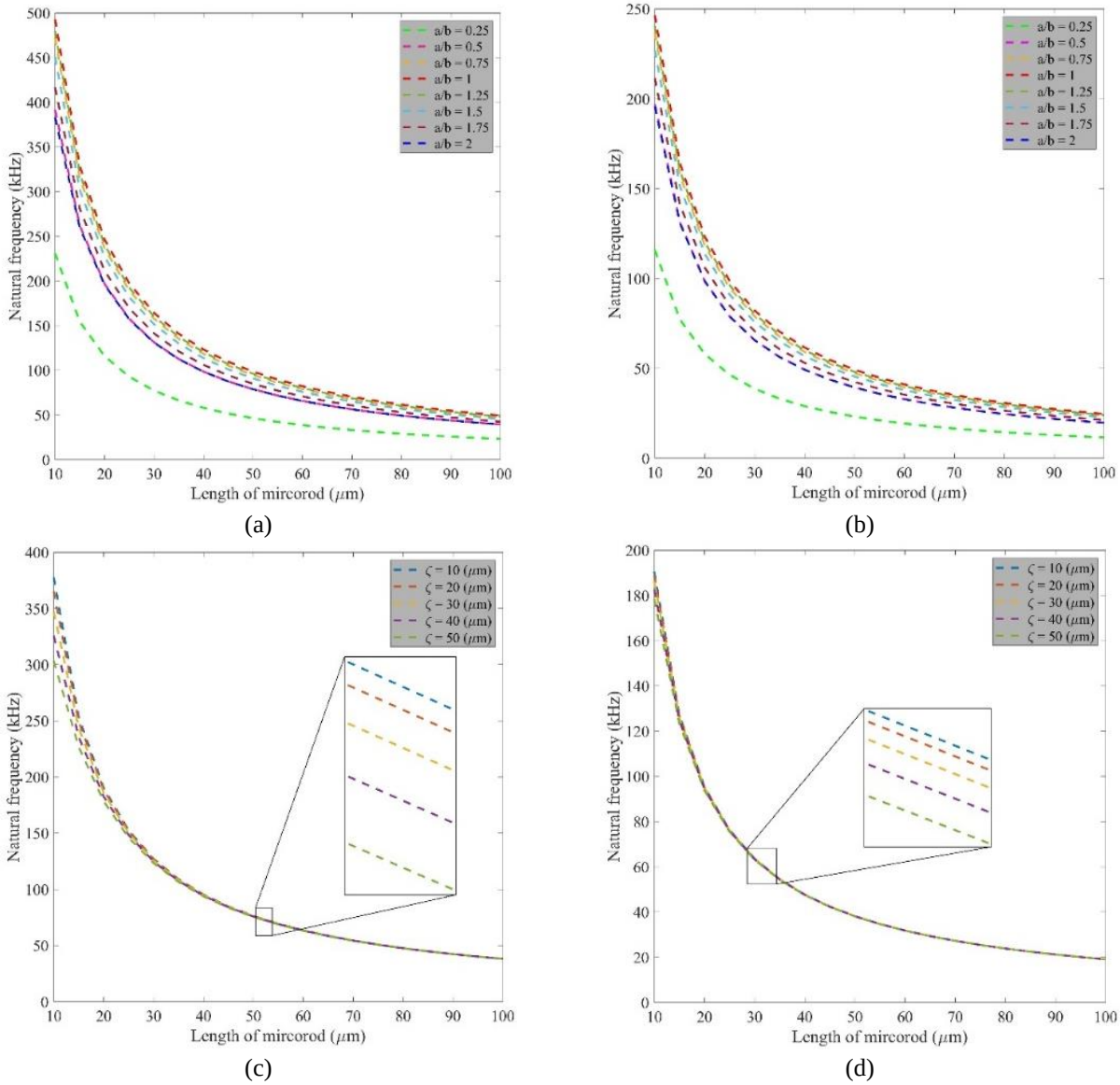

Fig. 6 Variation of the natural frequency versus length of microrod for various geometry values for elliptical cross-section under (a) C-C (b) C-F boundary conditions and triangular cross-section (c) C-C (d) C-F boundary conditions

under torsional vibration. We analyzed triangular and elliptical shapes using nonlocal strain gradient theory to capture subtle effects at small scales. The results indicate that:

• Raising the nonlocal parameter (μ) reduces the natural frequencies due to the stiffness-softening effect from small-scale interactions.

• The aspect ratio (a/b) and cross-sectional shape greatly affect the dynamic response, elliptical microrods showed higher frequencies than triangular microrods because of their greater polar moment of inertia.

• Boundary constraints greatly affect vibrational properties. The C–C setup generated higher frequencies than the C–F setup due to increased stiffness at both ends.

• An increase in natural frequencies was attributed to the length-scale parameter, emphasizing the notable size-dependent effects accounted for by NSGT.

• An inverse relationship was observed between microrod length and natural frequency, with shorter rods exhibiting increased stiffness and higher vibrational modes.

The study demonstrates that the dynamic behavior of auxetic microrods is significantly affected by the synergistic influence of geometric configuration, boundary conditions, and scale-dependent parameters. These findings highlight that changing microstructural features can help control dynamic behavior, which is important for designing lightweight, vibration-resistant auxetic parts for protective gear like shin guards.

Although the present investigation focuses on auxetic microrods derived from a single type of re-entrant honeycomb geometry with varying inclined angles, the framework established here can be readily extended to other auxetic topologies such as chiral, rotating-square, or star-shaped lattices. These geometries achieve a negative Poisson's ratio through different ways they deform, which can result in varied stiffness–frequency relationships and

energy absorption. The numerical results from this study help explain how acoustic geometries and microscale features work together to influence vibration response. This knowledge can help make protective structures work better in practice. Future studies should therefore explore how these alternative auxetic unit-cell designs influence the torsional and coupled vibration responses at the microscale, to further generalize the present findings and broaden their applicability in multifunctional metamaterial design.

References

Alghanmi, R.A. (2025), "Size-dependent static response of a functionally graded nanobeam attached to a piezoelectric fibre-reinforced composite actuator", *Sci. Rep.*, **15**(1), 28734. https://doi.org/10.1038/s41598-025-13726-5.

Alkunte, S., Fidan, I., Naikwadi, V., Gudavasov, S., Ali, M.A., Mahmudov, M., Hasanov, S. and Cheepu, M. (2024), "Advancements and challenges in additively manufactured functionally graded materials: A comprehensive review", *J. Manuf. Mater. Proc.*, **8**(1). https://doi.org/10.3390/jmmp8010023

Alkunte, S., Gupta, M., Rajeshirke, M., More, N., Cheepu, M., Gupta, A., Lakal, N., Shingare, K., Alifui-Segbaya, F. and Fidan, I. (2024), "Functionally graded metamaterials: Fabrication techniques, modeling, and applications—A review", *Processes*, **12**(10). https://doi.org/10.3390/pr12102252

Arda, M. (2021), "Axial dynamics of functionally graded Rayleigh-Bishop nanorods", *Microsyst. Technol.*, **27**(1), 269-282. https://doi.org/10.1007/s00542-020-04950-2.

Arefi, M. and Amabili, M. (2021), "A comprehensive electro-magneto-elastic buckling and bending analyses of three-layered doubly curved nanoshell, based on nonlocal three-dimensional theory", *Compos. Struct.*, **257**, 113100. https://doi.org/10.1016/j.compstruct.2020.113100.

Bağdatlı, S.M. (2015), "Non-linear vibration of nanobeams with various boundary condition based on nonlocal elasticity theory", *Compos. Part B Eng.*, **80**, 43-52. https://doi.org/10.1016/j.compositesb.2015.05.030.

Beitollahi, A., Janghorban, M., Bazargan-Lari, Y. and Tounsi, A. (2025), "On the variable length scale parameter for agglomeration of nanoparticles in nanocomposites", *Proceedings of the Institution of Mechanical Engineers, Part C: Journal of Mechanical Engineering Science*, **239**(10), 3828-3850. https://doi.org/10.1177/09544062241308513.

Boulahbal, Y., Bouzid, T., Mamen, B., Bouhadra, A., Boutrid, A., Tounsi, A. and Benrahou, K.H. (2025), "On the bending behavior of nonhomogeneous nanoscale beams under nonlinear hygro-thermo-mechanical loading", *Acta Mechanica*, **236**(5), 2921-2941. https://doi.org/10.1007/s00707-025-04293-x.

Bousmaha, K., Belalia, S.A., Chorfi, S.M., Tounsi, A., Al-Osta, M.A. and Alluqmani, A.E. (2025), "On the dynamic behavior of plates made of porous advanced materials reinforced with carbon nanotubes using a p-version of finite element method", *Mech. Based Des. Struct.*, 1-30. https://doi.org/10.1080/15397734.2025.2534679.

Boussalem, M., Bouhadra, A., Menasria, A., Mamen, B., Refrafi, S., Tounsi, A., Bousahla, A.A. and Mahmoud, S.R. (2025), "Analytic solution for the hygro-thermo-mechanical bending behaviour of FG nanoplates on nonlinear elastic foundations using a nonlocal Quasi-3D HSDT", *Struct. Eng. Mech.*, **95**(2), 137-153. https://doi.org/10.12989/SEM.2025.95.2.137.

Challamel, N., Kaci, A. and Tounsi, A. (2025), "Exact solutions for the static bending of nonlocal higher-order shear beams under various boundary conditions", *Mech. Adv. Mater. Struct.*, 1-17. https://doi.org/10.1080/15376494.2025.2521837.

Chang, Z., Wang, K., Wan, Y., Habibi, M., Bouallegue, B. and Chen, X. (2025), "Hemodynamic responses to physical activity: Numerical analysis of dynamic behavior in microvascular structures under exercise-induced forces", *Adv. Nano Res.*, **18**(3), 265-280. https://doi.org/10.12989/anr.2025.18.3.265.

Chen, C., Xiao, X., Chen, L., Habibi, M., Brahmia, A. and Chen, X. (2025), "Exercise-induced changes in protein tissue stability in athletes via biomechanical analysis using size-dependent mechanical models", *Adv. Nano Res.*, **18**(5), 419-432. https://doi.org/10.12989/.2025.18.5.419.

Chen, H., Zhu, J., Habibi, M., Brahmia, A. and Wnag, D. (2025), "Stability analysis of nano-devices: Exercise-mediated effects on nanodevice stability in drug delivery applications", *Adv. Nano Res.*, **18**(5), 445-458. https://doi.org/10.12989/anr.2025.18.5.445.

Cuong-Le, T., Nguyen, K.D., Le-Minh, H., Phan-Vu, P., Nguyen-Trong, P. and Tounsi, A. (2022), "Nonlinear bending analysis of porous sigmoid FGM nanoplate via IGA and nonlocal strain gradient theory", *Adv. Nano Res.*, **12**(5), 441-455. https://doi.org/10.12989/anr.2022.12.5.441.

Dai, Y., Jiang, Z., Chen, K.Y., Zuo, D., Habibi, M., Ali, H.E. and Albaijan, I. (2022), "Geometry impact on the stability behavior of cylindrical microstructures: Computer modeling and application for small-scale sport structures", *Steel Compos. Struct.*, **48**(4), 443-459. https://doi.org/10.12989/scs.2023.48.4.443.

Daichang, Z., Aiyun, L., Zhiqiang, S., Habibi, M., Albaijan, I. and Wong, L. (2025), "Dynamic stability and vibration responses of a volleyball game ball", *Adv. Nano Res.*, **18**(4), 321-335. https://doi.org/10.12989/anr.2025.18.4.321.

Ebrahimi, F., Seyfi, A. and Dabbagh, A. (2019), "Dispersion of waves in FG porous nanoscale plates based on NSGT in thermal environment", *Adv. Nano Res.*, **7**(5), 325-335. https://doi.org/10.12989/ANR.2019.7.5.325.

Eipakchi, H. and Mahboubi Nasrekani, F. (2020), "Vibrational behavior of composite cylindrical shells with auxetic honeycombs core layer subjected to a moving pressure", *Composite Structures*, **254**, 112847. https://doi.org/10.1016/j.compstruct.2020.112847.

Faghidian, S. A. and Tounsi, A. (2022), "Dynamic characteristics of mixture unified gradient elastic nanobeams", *Facta Universitatis, Series: Mechanical Engineering*, **20**(3). https://doi.org/10.22190/FUME220703035F

Fang, J., Ma, D., Fei, X. and Habibi, M. (2025), "Strengthening the mechanical properties of 3D printed thermoplastic elastomer by blending with acrylonitrile butadiene styrene, polypropylene and polyethylene", *Physica Scripta*, **100**(4), 045922. https://doi.org/10.1088/1402-4896/adbc2e.

Gartia, A.K. and Chakraverty, S. (2025), "Advanced computational modeling and mechanical behavior analysis of multi-directional functionally graded nanostructures: a comprehensive review", *Comput. Model. Eng. Sci.*, **142**(3). https://doi.org/10.32604/cmes.2025.061039.

Gheshlaghi, B. and Hasheminejad, S.M. (2011), "Surface effects on nonlinear free vibration of nanobeams", *Compos. Part B Eng.*, **42**(4), 934-937. https://doi.org/10.1016/j.compositesb.2010.12.026.

Hajmohammad, M. H., Kolahchi, R., Zarei, M. S. and Nouri, A. H. (2019), "Dynamic response of auxetic honeycomb plates integrated with agglomerated CNT-reinforced face sheets subjected to blast load based on visco-sinusoidal theory", *Int. J. Mech. Sci.*, **153-154**, 391-401. https://doi.org/10.1016/j.ijmecsci.2019.02.008.

Hu, Y., Zhao, W., An, Y., Liao, M., Habibi, M. and Yan, X. (2025), "Mechanical performance of auxetic rotational polygons metamaterials based on simple rectangular-shaped parts:

Experimental validation and FEA modeling", *Int. J. Struct. Stabil. Dyn.*, 2650344. https://doi.org/10.1142/S021945542650344X.

Huang, Y., Zhang, B., Sun, C., Habibi, M., Ghazouani, N. and El Ouni, M.H. (2025), "Wave responses in seismic FGM concrete nanobeam using deep neural network", *Adv. Nano Res.*, **18**(6), 503. https://doi.org/10.12989/ANR.2025.18.6.503.

Kadiri, A., Bendaida, M., Attia, A., Balubaid, M., Mahmoud, S.R., Bousahla, A.A., Tounsi, A., Bourada, F. and Tounsi, A. (2024), "Wave propagation in FG polymer composite nanoplates embedded in variable elastic medium", *Adv. Nano Res.*, **17**(3), 235-248. https://doi.org/10.12989/ANR.2024.17.3.235.

Kavousi Sisi, A., Ozherelkov, D., Chernyshikhin, S., Pelevin, I., Kharitonova, N. and Gromov, A. (2025), "Functionally graded multi-materials by laser powder bed fusion: A review on experimental studies", *Prog. Add. Manuf.*, **10**(4), 1843-1912. https://doi.org/10.1007/s40964-024-00739-1.

Koizumi, M. (1997), "FGM activities in Japan", *Compos. Part B Eng.*, **28**(1), 1-4. https://doi.org/10.1016/S1359-8368(96)00016-9.

Li, C., Shen, H.S. and Wang, H. (2018), "Nonlinear vibration of sandwich beams with functionally graded negative poisson's ratio honeycomb core", *Int. J. Struct. Stabil. Dyn.*, **19**(3), 1950034. https://doi.org/10.1142/S0219455419500342.

Li, C., Shen, H.S. and Wang, H. (2019), "Nonlinear bending of sandwich beams with functionally graded negative Poisson's ratio honeycomb core", *Compos. Struct.*, **212**, 317-325. https://doi.org/10.1016/j.compstruct.2019.01.020.

Li, X., Luo, L., Habibi, M. and Wang, L. (2025), "Extending a higher-order foldability constitutive model for dynamic response analysis of 3D-reinforced shell of deformable", *Acta Mechanica*, **236**(3), 1509-1533. https://doi.org/10.1007/s00707-024-04216-2.

Liu, G., Wu, S., Shahsavari, D., Karami, B. and Tounsi, A. (2022), "Dynamics of imperfect inhomogeneous nanoplate with exponentially-varying properties resting on viscoelastic foundation", *Eur. J. Mech. A Solids*, **95**, 104649. https://doi.org/10.1016/j.euromechsol.2022.104649.

Liu, J., Fu, Y., Habibi, M. and Sun, Y. (2025a), "Evaluation of mechanical behavior of textile microfibers", *Acta Mechanica*, **236**(5), 3081-3094. 10.1007/s00707-025-04314-9.

Liu, Q., Zhang, Y., Habibi, M., Brahmia, A. and Su, Y. (2025b), "The activity and technique principle of football shooting are investigated from the viewpoint of nano-bio-mechanics", *Adv. Nano Res.*, **18**(3), 241. https://doi.org/10.12989/anr.2025.18.3.241.

Liu, Y., Qin, Z. and Chu, F. (2021a), "Nonlinear forced vibrations of FGM sandwich cylindrical shells with porosities on an elastic substrate", *Nonlinear Dyn.*, **104**(2), 1007-1021. https://doi.org/10.1007/s11071-021-06358-7.

Liu, Y., Qin, Z. and Chu, F. (2021b), "Nonlinear forced vibrations of functionally graded piezoelectric cylindrical shells under electric-thermo-mechanical loads", *Int. J. Mech. Sci.*, **201**, 106474. https://doi.org/10.1016/j.ijmecsci.2021.106474.

Liu, Y., Qin, Z. and Chu, F. (2022), "Nonlinear forced vibrations of rotating cylindrical shells under multi-harmonic excitations in thermal environment", *Nonlinear Dyn.*, **108**(4), 2977-2991. https://doi.org/10.1007/s11071-022-07449-9.

Nasrekani, F.M., Eipakchi, H., Mala, K.A., Micky, C. and Narayan, S. (2025), "Experimental and analytical study of initial condition effects on nonlinear vibrations of thin-walled beams", *Experim. Tech.*, 1-13. https://doi.org/10.1007/s40799-025-00829-x.

Palani, V. and Swain, A. (2025), "Nonlinear vibration analysis of composite and functionally graded material shell structures: A literature review from 2013 to 2023", *Int. J. Nonlinear Mech.*, **168**, 104939. https://doi.org/10.1016/j.ijnonlinmec.2024.104939.

Pradhan, S.C. and Phadikar, J.K. (2009), "Nonlocal elasticity theory for vibration of nanoplates", *J. Sound Vib.*, **325**(1), 206-223. https://doi.org/10.1016/j.jsv.2009.03.007.

Qin, Z., Zhao, S., Pang, X., Safaei, B. and Chu, F. (2020), "A unified solution for vibration analysis of laminated functionally graded shallow shells reinforced by graphene with general boundary conditions", *Int. J. Mech. Sci.*, **170**, 105341. https://doi.org/10.1016/j.ijmecsci.2019.105341.

Qing, T.D. and Zhi, C.Y. (2010), "Wave propagation in sandwich panel with auxetic core", *J. Solid Mech.*, **2**(4), 393-402.

Seyfi, A., Teimouri, A. and Ebrahimi, F. (2024), "Scale-dependent torsional vibration response of non-circular nanoscale auxetic rods", *Waves Random Complex Med.*, **34**(5), 4425-4441. https://doi.org/10.1080/17455030.2021.1990441.

Sokolnikoff, I.S. and Specht, R.D. (1956), *Mathematical Theory of Elasticity*, 83, McGraw-Hill New York, U.S.A.

Van Vinh, P. and Tounsi, A. (2022a), "Free vibration analysis of functionally graded doubly curved nanoshells using nonlocal first-order shear deformation theory with variable nonlocal parameters", *Thin Walled Struct.*, **174**, 109084. https://doi.org/10.1016/j.tws.2022.109084.

Van Vinh, P. and Tounsi, A. (2022b), "The role of spatial variation of the nonlocal parameter on the free vibration of functionally graded sandwich nanoplates", *Eng. Comput.*, **38**(5), 4301-4319. https://doi.org/10.1007/s00366-021-01475-8.

Van Vinh, P. and Zenkour, A.M. (2025), "Vibration analysis of functionally graded sandwich porous plates with arbitrary boundary conditions: a new general viscoelastic Winkler–Pasternak foundation approach", *Eng. Comput.*, 1-29. https://doi.org/10.1007/s00366-025-02106-2.

Wan, Y., Zhang, G., Chang, Z., Habibi, M., Albaijan, I. and Li, Y. (2025), "Advancing sports equipment performance: Leveraging rotating small-scale structures for enhanced athletic tools", *Adv. Nano Res.*, **18**(5), 467-480. https://doi.org/10.12989/anr.2025.18.5.467.

Wang, J., Pu, Q., Ning, P. and Lu, S. (2021), "Activated carbon-based composites for capturing CO2: A review", *Greenhouse Gases Sci. Tech.*, **11**(2), 377-393. https://doi.org/10.1002/ghg.2051.

Wang, J., Qian, C., Zhang, F., Qiu, X., Yu, B., Shi, J. and Chen, J. (2025), "Experimental and numerical analysis of functionally graded hybrid TPMS heat exchangers for enhanced flow and thermal performance", *Appl. Therm. Eng.*, **264**, 125528. https://doi.org/10.1016/j.applthermaleng.2025.125528.

Xia, L., Habibi, M. and Li, Q. (2025), "Computational stability analysis of sport structures: Importance of MEMS for testing athlete performance", *Steel Compos. Struct.*, **54**(1), 53. https://doi.org/10.12989/scs.2025.54.1.053.

Xiao, D., Habibi, M., Bouallegue, B. and Bagheri, M. (2025), "A pathway to sports innovation through the stability performance of lightweight functionally graded tubular structures", *Adv. Nano Res.*, **18**(4), 337-350. https://doi.org/10.12989/anr.2025.18.4.337.

Xiao, H., Habibi, M. and Habibi, M. (2024), "Bulk wave propagation analysis of imperfect FG bio-composite beams resting on variable elastic medium", *Mater. Today Commun.*, **39**, 108524. https://doi.org/10.1016/j.mtcomm.2024.108524.

Xu, L., Zhang, C., Habibi, M., Albaijan, I. and Yin, C. (2025), "Research on applicable sensor for solving the volleyball sport problem using smart nanomaterial based on dynamic simulation", *Adv. Nano Res.*, **18**(5), 405-417. https://doi.org/10.12989/anr.2025.18.5.405.

YaJie, Z., Meng, W., Zhiqiang, S., Habibi, M., Brahmia, A. and Albaijan, I. (2025), "Wave propagation response of porous vibrating sports equipment under thermal loading application on testing athlete performance", *Steel Compos. Struct.*, **55**(2), 143-

157. https://doi.org/10.12989/scs.2025.55.2.143.
Yang, L., Liu, L., Habibi, M. and Chen, Z. (2025), "Enhancing sports equipment performance: Development of polyvinyl chloride-based nanocomposites with plantain wood powder and nano clay", *Adv. Nano Res.*, **18**(4), 351-360. https://doi.org/10.12989/anr.2025.18.4.351.
Yu, H., Habibi, M., Motamedi, K., Semirumi, D. T. and Ghorbani, A. (2023), "Utilizing stem cells in reconstructive treatments for sports injuries: An innovative approach", *Tissue Cell*, **83**, 102152. https://doi.org/10.1016/j.tice.2023.102152.
Yuanchao, H., Yijiang, W., Habibi, M., Zhicong, D., Bei, L. and Yuhuan, L. (2025), "On propagation analysis of flexural waves in functionally graded poroelastic biocomposite higher-order beams", *Acta Mechanica*, **236**(7), 3959-3974. https://doi.org/10.1007/s00707-025-04362-1.
Yuanchao, H., Yunzhu, A., Shangmao, H., Habibi, M., Lei, G. and Ying, C. (2025), "Humid-thermal environment influence on dispersion of waves in sigmoid poroelastic cylindrical panels resting on sinusoidal elastic foundation", *Mech. Based Des. Struct.*, 1-19. https://doi.org/10.1080/15397734.2025.2491027.
Zarezadeh, E., Hosseini, V. and Hadi, A. (2020), "Torsional vibration of functionally graded nano-rod under magnetic field supported by a generalized torsional foundation based on nonlocal elasticity theory", *Mech. Based Des. Struct.*, **48**(4), 480-495. https://doi.org/10.1080/15397734.2019.1642766.
Zhang, Y., Xu, L., Wang, J., Pan, H., Dou, M., Teng, Y., Fu, X., Liu, Z., Huang, X. and Wang, M. (2025), "Bagasse-based porous flower-like MoS2/carbon composites for efficient microwave absorption", *Carbon Lett.*, **35**(1), 145-160. https://doi.org/10.1007/s42823-024-00832-z.
Zhao, W., Yan, A., Su, Z., Huang, F., Wang, Q., Li, S., Lu, S., Wang, C., Zhang, T., Zhang, J., Gao, Y. and Yuan, H. (2024), "Multiobjective-optimization MoS2/Cd-ZnIn2S4/CdS composites prepared by in situ structure-tailored technique for high-efficiency hydrogen generation", *Small Struct.*, **5**(7), 2300569. https://doi.org/10.1002/sstr.202300569.
Zhu, D., Zhang, A., Habibi, M. and Arefi, M. (2025), "Electroelastic analysis of piezoelectric double curved-shells for spring board practice and gymnastic training via Levy-Type Method", *Steel Compos. Struct.*, **55**(2), 97. https://doi.org/10.12989/scs.2025.55.2.351.

CC